
Compact Approximation for Polynomial of Covariance Feature

Yusuke Mukuta

The University of Tokyo, RIKEN AIP
mukuta@mi.t.u-tokyo.ac.jp

Tatsuaki Machida

The University of Tokyo
machida@mi.t.u-tokyo.ac.jp

Tatsuya Harada

The University of Tokyo, RIKEN AIP
harada@mi.t.u-tokyo.ac.jp

Abstract

Covariance pooling is a feature pooling method with good classification accuracy. Because covariance features consist of second-order statistics, the scale of the feature elements are varied. Therefore, normalizing covariance features using a matrix square root affects the performance improvement. When pooling methods are applied to local features extracted from CNN models, the accuracy increases when the pooling function is back-propagatable and the feature-extraction model is learned in an end-to-end manner. Recently, the iterative polynomial approximation method for the matrix square root of a covariance feature was proposed, and resulted in a faster and more stable training than the methods based on singular-value decomposition. In this paper, we propose an extension of compact bilinear pooling, which is a compact approximation of the standard covariance feature, to the polynomials of the covariance feature. Subsequently, we apply the proposed approximation to the polynomial corresponding to the matrix square root to obtain a compact approximation for the square root of the covariance feature. Our method approximates a higher-dimensional polynomial of a covariance by the weighted sum of the approximate features corresponding to a pair of local features based on the similarity of the local features. We apply our method for standard fine-grained image recognition datasets and demonstrate that the proposed method shows comparable accuracy with fewer dimensions than the original feature.

1 Introduction

Feature pooling is a method to summarize the statistics of local features extracted from one image into one global feature. Earlier, feature pooling was applied to handcrafted features such as SIFT [14] and HOG [1]. Currently, feature pooling methods are applied to activate the convolutional layers of convolutional neural networks (CNNs) such as VGG-Net [17] and ResNet [5] to improve classification accuracy.

Among the feature pooling methods, bilinear pooling [13] that uses second-order statistics as a global feature demonstrates good accuracy, and various extensions of bilinear pooling have been proposed.

One problem of the original bilinear pooling is its dimension. The dimensionality of bilinear pooling is the squared order of the dimensionality of local features. This is problematic particularly when bilinear pooling is applied to CNN features because they tend to be high-dimensional. To reduce the feature dimension, compact bilinear pooling [3] exploits the tensor sketch [16] and random Macraulin [8] approximations for polynomial kernels to construct a differentiable pooling layer. Compact bilinear pooling demonstrates a comparable accuracy to bilinear pooling with fewer dimensions.

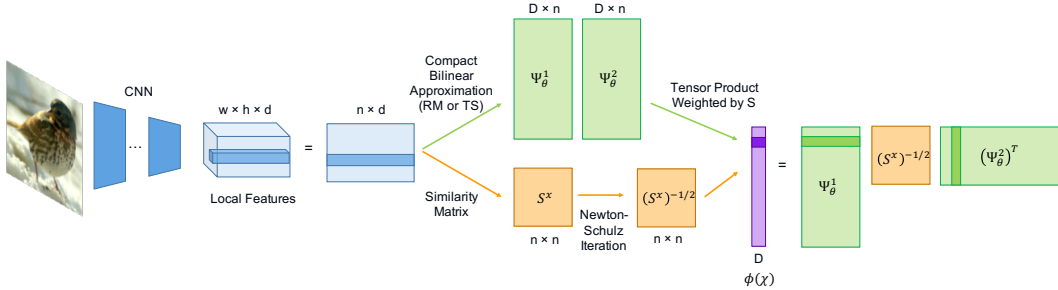


Figure 1: Overview of the proposed feature coding method. We first extract CNN local feature $\mathcal{X} = \{x_n\}_{n=1}^{n_x}$. We subsequently calculate $\Psi^i(\mathcal{X})$, S^x and $(S^x)^{-1/2}$. We finally calculate $(S^x)^{-1/2}$ -weighted sum of products of $\Psi^1(\mathcal{X})$ and $\Psi^2(\mathcal{X})$ as a global feature.

Another problem is that the feature is affected by the elements of local features with large values because bilinear pooling uses second-order information. Improved bilinear pooling [12] applies matrix square root normalization to alleviate this problem. Matrix square root normalization is a method that uses 1/2 power of a bilinear feature as a global feature. Because a bilinear feature is positive semi-definite, we can calculate the matrix square root normalization by first applying singular-value decomposition (SVD) and subsequently multiplying the singular matrices with 1/2 power of the singular values. The original improved bilinear pooling and its variant [11] calculate the backpropagation of matrix square root normalization using matrix backpropagation [7] through the differential with respect to the singular values and singular vectors. These methods exhibit slowness and instability in SVD calculations on a GPU. Furthermore, when different singular values have the same value, the decomposition is not unique and, thus, we cannot compute the differential, thus resulting in the failure of computation of backpropagation. Recently, the iSQRT-COV [10] proposed avoiding SVD calculation using the approximation of 1/2 power of matrices with Newton-Schulz Iteration [6]. Newton-Schulz Iteration approximates the 1/2 power of matrices with only the summation and multiplication of matrices; thus, this method is compatible with the GPU computation and CNN learning framework. Furthermore, the approximated matrices are the polynomials of the input matrices. iSQRT-COV demonstrated good recognition accuracy with fast computation.

Based on these studies, we propose a novel extension of the bilinear pooling layer that is compact, normalized, and easy to calculate backpropagation. Hence, we propose a compact approximation for the bilinear feature with iterative matrix square root normalization. Because matrix square root normalization can be approximated using a polynomial, we first propose an approximation for a general polynomial of the bilinear feature. We calculate the approximation by first representing the polynomial of a covariance using the weighted sum of a bilinear feature that corresponds to a pair of local features, and subsequently calculate the weight and approximation for each bilinear feature. We then apply the proposed method to the polynomial corresponding to the 1/2 power to obtain the approximate feature for matrix square root normalization. Because we can use Newton-Schulz Iteration to calculate the weights of summation, we avoid SVD for our approximation method. We plot the overview of the proposed method in Figure 1.

We applied the proposed approximation method to ResNet and evaluated the methods on standard fine-grained image recognition datasets. Our method exhibited better accuracy than the existing compact approximation methods and demonstrated comparable accuracy with the original normalized covariance features.

Our contributions are as follows:

- We proposed a novel extension of bilinear pooling that approximates the square root of the covariance feature with low dimension via Newton-Schulz Iteration.
- We evaluated the proposed method on standard fine-grained image recognition datasets and confirmed that our method demonstrates comparable performance to the iSQRT-COV with lower dimension and with lower computation time than Monet.

Algorithm 1 Calculate tensor sketch approximation [3]

Require: $\mathcal{X} = \{x_n\}_{n=1}^{n_x}$, where $x_n \in \mathbb{R}^d$, feature dimension D

Ensure: $\phi^{\text{TS}}(\mathcal{X}) \in \mathbb{R}^D$

Generate uniform random $h_k \in \{1, 2, \dots, D\}^d$ and $s_k \in \{1, -1\}^d$ for $k = 1, 2$

Define $\psi^{\text{TS}}(x, h, s) = \{(Qx)_1, \dots, (Qx)_D\}$ where $(Qx)_j = \sum_{\{i \in \{1, 2, \dots, d\} | h(i)=j\}} s(i)x^i$

$\phi^{\text{TS}}(\mathcal{X}) = \sum_{n=1}^{n_x} \text{fft}^{-1}(\text{fft}(\psi^{\text{TS}}(x_n, h_1, s_1) \circ (\psi^{\text{TS}}(x_n, h_2, s_2))))$

Algorithm 2 Calculate random Maclaurin approximation [3]

Require: $\mathcal{X} = \{x_n\}_{n=1}^{n_x}$, where $x_n \in \mathbb{R}^d$, feature dimension D

Ensure: $\phi^{\text{RM}}(\mathcal{X}) \in \mathbb{R}^D$

Generate uniform random $W_k \in \{1, -1\}^{D \times d}$ for $k = 1, 2$

$\phi^{\text{RM}}(\mathcal{X}) = \frac{1}{\sqrt{D}} \sum_{n=1}^{n_x} (W_1 x_n) \circ (W_2 x_n)$

2 Related Work

We review the existing studies regarding bilinear pooling in this section. We first explain the original bilinear pooling, followed by its compact approximation and the meaning of approximation. Finally, we describe the variants that apply matrix square root normalization to match the scale of the feature elements.

When d -dimensional local descriptors $\mathcal{X} = \{x_n\}_{n=1}^{n_x}$ are available, where $x_n \in \mathbb{R}^d$, bilinear pooling [13] uses second-order statistics

$$C_x = \sum_{n=1}^{n_x} x_n x_n^t, \quad (1)$$

as a global image feature. Because Eq. (1) can be calculated using matrix multiplication, it is easy to calculate the differential; thus, we can learn the whole feature extraction network using backpropagation. The feature dimension of bilinear pooling is $O(d^2)$, which is large. Therefore, Gao et al. proposed its compact approximation called compact bilinear pooling [3] using techniques for approximating polynomial kernels, called tensor sketch [16] and random Macraulin [8]. This approximation implies the approximation in expectation. In other words, when we have another local descriptor $\mathcal{Y} = \{y_n\}_{n=1}^{n_y}$, where $y_n \in \mathbb{R}^d$ and its bilinear feature C_y and a feature function ϕ exists that maps a set of local features to \mathbb{R}^D parameterized by θ , in addition to the distribution p of θ that satisfies

$$\langle C_x, C_y \rangle = E_{\theta \sim p}[\langle \phi_\theta(\mathcal{X}), \phi_\theta(\mathcal{Y}) \rangle], \quad (2)$$

we can sample θ from p and use $\phi_\theta(\mathcal{X})$ as an approximation for C_x . We can obtain the compact feature by setting $D < d^2$. We describe the algorithm for compact bilinear pooling using both tensor sketch and random Macraulin in Algorithm 1, 2, where fft implies a fast Fourier transform and \circ implies an element-wise product. Both ϕ^{TS} and ϕ^{RM} satisfy the above equality. Our goal is to obtain ϕ_θ and p that approximate $\langle q(C_x), q(C_y) \rangle$ for any polynomial q .

Because a bilinear feature is a second-order statistics, improved bilinear pooling [12] applies matrix square root normalization to the bilinear feature C_x and uses $C_x^{1/2}$ as a global feature to alleviate the effect of feature elements with large values and cause the scale of each feature element to be similar. This normalized feature is more compatible with linear classifiers and thus results in higher accuracy. To calculate the backpropagation of a matrix square root, improved bilinear pooling calculates the strict square root using SVD or the approximate square root using Newton–Schulz Iteration [6] for forward calculation and solve the Lyapunov equation using SVD for the backward calculation. Liu et al. [11] proposed a direct backward calculation using the differential with respect to singular values and singular vectors. Furthermore, Liu et al. indicated that matrix square root normalization is the robust estimator of a covariance feature as well as the approximation of the Riemannian geometry in the space of positive definite matrices. G2DeNet [18] used both first- and second-order statistics as a global feature to represent information corresponding to a Gaussian distribution. Because these methods use SVD for the backward calculation, they suffer from computation overhead for GPU calculations and instability when the singular values are similar. Monet [4] proposed a compact

Table 1: Comparison of extended bilinear pooling methods.

Method	Compact	Matrix Normalization	Avoid SVD
Compact Bilinear Pooling [3]	✓	×	✓
Improved Bilinear Pooling [12]	×	✓	×
Monet [4]	✓	✓	×
iSQRT-COV [10]	×	✓	✓
Our work	✓	✓	✓

approximation for improved bilinear feature. Given the G2DeNet feature M , Monet first calculated the matrix Y that satisfied $M^{1/2} = Y^t Y$ using SVD. This Y exhibits the property where bilinear features calculated from the row vectors of Y become $M^{1/2}$. Therefore, compact bilinear pooling calculated from row vectors of Y approximates $M^{1/2}$. However, Monet required SVD for forward calculation with respect to Y . Li et al. [10] proposed a method iSQRT-COV that used Newton–Schulz Iteration for both forward and backward calculations. We can perform forward and backward calculations using GPU-friendly matrix multiplications to yield fast computation and improvement in accuracy.

We summarize the comparison of our method and existing methods in Table 1.

3 Proposed Method

We describe the proposed method in this section. Because matrix square root normalization is approximated by the polynomial of the input covariance matrix, in Section 3.1, we propose the approximation for any polynomial of covariance. In Section 3.2, we combine our proposed method to Newton–Schulz Iteration to obtain the approximation for matrix square root normalization with a small number of iterations.

3.1 Approximation for polynomial of bilinear feature

Given the local features $\mathcal{X} = \{x_n\}_{n=1}^{n_x}$, $\mathcal{Y} = \{y_n\}_{n=1}^{n_y}$, bilinear feature C_x, C_y was calculated using Eq. (1) and the polynomial q ; our goal is to calculate the feature function ϕ_θ and the distribution p of θ that satisfies

$$\langle q(C_x), q(C_y) \rangle = E_{\theta \sim p}[\langle \phi_\theta^q(\mathcal{X}), \phi_\theta^q(\mathcal{Y}) \rangle]. \quad (3)$$

This equation is an extension of Eq. (2), where we apply q on the left-hand side. In our experiment, we used the polynomial of the covariance instead of the polynomial of the bilinear feature to match the setting with iSQRT-COV. We can calculate the approximation by substituting $\frac{1}{\sqrt{n_x}} \left(x_n - \frac{1}{n_x} \sum_{n=1}^{n_x} x_n \right)$ for x_n . Furthermore, we can approximate the Gaussian embedding such as G2DeNet by substituting $\frac{1}{\sqrt{n_x}} \begin{pmatrix} x_n^t & 1 \end{pmatrix}^t$ for x_n .

Our primary result is as follows.

Proposition 1. *We assume that q is written as $q(x) = b + xr(x)$, where b is a bias term and r is a polynomial; $\langle x_m x_n^t, y_o y_p^t \rangle$ is approximated as a bilinear form of ψ_θ , written as*

$$\langle x_m x_n^t, y_o y_p^t \rangle = E_{\theta \sim p}[\langle U(\psi_\theta^1(x_m) \otimes \psi_\theta^2(x_n)), U(\psi_\theta^1(y_o) \otimes \psi_\theta^2(y_p)) \rangle], \quad (4)$$

for $1 \leq m, n \leq n_x$ and $1 \leq o, p \leq n_y$, where \otimes denotes the Kronecker product and U is the deterministic weight matrix. Furthermore, we denote the matrices that we concatenate, $\psi_\theta^i(x_n)$ and $\psi_\theta^i(y_n)$, as $\Psi^i(\mathcal{X}) \in \mathbb{R}^{D \times n_x}$ and $\Psi^i(\mathcal{Y}) \in \mathbb{R}^{D \times n_y}$, respectively. Then, it follows that

$$\begin{aligned} & \langle q(C_x), q(C_y) \rangle \\ &= E_{\theta \sim p}[\langle c + \sum_{n_1=1}^{n_x} U((\Psi_\theta^1(\mathcal{X})r(S^x))_{:,n_1} \otimes \psi_\theta^2(x_{n_1})), c + \sum_{n_1=1}^{n_y} U((\Psi_\theta^1(\mathcal{Y})r(S^y))_{:,n_1} \otimes \psi_\theta^2(y_{n_1})) \rangle], \end{aligned} \quad (5)$$

where $A_{:,n}$ is the n -th column vector for matrix A ; c is a vector calculated using d -dimensional element vectors e_i as $c = b \sum_{i=1}^d U(\psi_\theta^1(e_i) \otimes \psi_\theta^2(e_i))$ and $S_{n_1 n_2}^x = \langle x_{n_1}, x_{n_2} \rangle$, $S_{n_1 n_2}^y = \langle y_{n_1}, y_{n_2} \rangle$.

From this proposition, we can calculate the approximate feature as follows:

$$\phi_\theta^q(\mathcal{X}) = c + \sum_{n_1=1}^{n_x} U \left((\Psi_\theta^1(\mathcal{X})r(S^x))_{:,n_1} \otimes \psi_\theta^2(x_{n_1}) \right). \quad (6)$$

In addition to the feature calculated by compact bilinear pooling, our feature exploits the constant vector c that corresponds to the bias term and the approximate features that correspond to the pair of local features with the weight $r(S^x)_{n_1 n_2}$.

Before we proceed to the proof, we present some noteworthy points. First, we can decompose $q(x) = b + xr(x)$ for any polynomial q by setting b as the constant term of q and r as the terms with degree higher than 0 divided by x . Eq. (4) is the generalization of the tensor sketch and random Macraulin. For example, we derive the random Macraulin from this equation by setting $\psi^i(x) = W_i x$ and U as a matrix corresponding to the mapping from the Kronecker product to the element-wise product divided by \sqrt{D} . Additionally, we derive the tensor sketch by setting $\psi^i(x) = \text{fft}(\psi^{\text{TS}}(x_n, h_i, s_i))$ and U as the composition of the matrix that corresponds to the fast Fourier transform and the matrix that corresponds to the mapping from the Kronecker product to the element-wise product. The implementation follows the original approximation method. We make this assumption to avoid the calculation of approximate features for all the n^2 pair of local features by exploiting bilinearity. Furthermore, because the summation weight $r(S^x)$ does not depend on θ and is fixed, the variance and concentration inequality of the proposed feature can be calculated straightforwardly from those of the original approximated feature.

Proof. First, the monomial of C_x can be represented using x_n and S^x as follows:

Lemma 1. *when we assume $n > 0$, it follows that*

$$C_x^m = \sum_{n_1=1}^{n_x} \sum_{n_2=1}^{n_x} (S^x)_{n_1, n_2}^{m-1} x_{n_1} x_{n_2}^t, \quad (7)$$

This lemma can be proved by induction with respect to n . From this lemma, we can prove the case for the monomials.

Lemma 2. *When we assume Eq. (4) and $n, m > 0$, it follows that*

$$\begin{aligned} \langle C_x^m, C_y^n \rangle = E_{\theta \sim p} [& \langle \sum_{n_1=1}^{n_x} \sum_{n_2=1}^{n_x} (S^x)_{n_1, n_2}^{m-1} U(\psi_\theta^1(x_{n_1}) \otimes \psi_\theta^2(x_{n_2})), \\ & \sum_{n_1=1}^{n_y} \sum_{n_2=1}^{n_y} (S^y)_{n_1, n_2}^{n-1} U(\psi_\theta^1(y_{n_1}) \otimes \psi_\theta^2(y_{n_2})) \rangle], \end{aligned} \quad (8)$$

This lemma follows from the fact that

$$\langle C_x^m, C_y^n \rangle = \sum_{n_1=1}^{n_x} \sum_{n_2=1}^{n_x} \sum_{n_3=1}^{n_y} \sum_{n_4=1}^{n_y} (S^x)_{n_1, n_2}^{m-1} (S^y)_{n_3, n_4}^{n-1} \langle x_{n_1} x_{n_2}^t, y_{n_3} y_{n_4}^t \rangle, \quad (9)$$

and Eq. (4). Next, we calculate the case when one term is constant.

Lemma 3. *When we assume Eq. (4) and $m > 0$, it follows that*

$$\langle C_x^m, I_d \rangle = E_{\theta \sim p} [\langle \sum_{n_1=1}^{n_x} \sum_{n_2=1}^{n_x} (S^x)_{n_1, n_2}^{m-1} U(\psi_\theta^1(x_{n_1}) \otimes \psi_\theta^2(x_{n_2})), \sum_{j=1}^d U(\psi_\theta^1(e_j) \otimes \psi_\theta^2(e_j)) \rangle], \quad (10)$$

where I_d is the d -dimensional identity matrix. This follows from the fact that I_d is a bilinear feature of e_i s because $I_d = \sum_{i=1}^d e_i e_i^t$. Finally, we calculate the case when both terms are constant.

Lemma 4. *It follows that*

$$\langle I_d, I_d \rangle = E_{\theta \sim p} [\sum_{j=1}^d U(\psi_\theta^1(e_j) \otimes \psi_\theta^2(e_j)), \sum_{j=1}^d U(\psi_\theta^1(e_j) \otimes \psi_\theta^2(e_j))], \quad (11)$$

Algorithm 3 Calculating the approximation for matrix square root of bilinear feature

Require: $\mathcal{X} = \{x_n\}_{n=1}^{n_x}$, where $x_n \in \mathbb{R}^d$, feature dimension D , iteration number k

Ensure: $\phi(\mathcal{X}) \in \mathbb{R}^D$

Calculate S^x where $S_{n_1 n_2}^x = \langle x_{n_1}, x_{n_2} \rangle$

$$A = \frac{1}{\text{trace} S^x} S^x$$

$$Y_0 = A, Z_0 = I_d$$

for $i = 0$ to $k - 1$ **do**

$$Y_{k+1} = \frac{1}{2} Y_k (3I_d - Z_k Y_k)$$

$$Z_{k+1} = \frac{1}{2} (3I_d - Z_k Y_k) Z_k$$

end for

$$S = \frac{1}{\sqrt{\text{trace} S^x}} Z_k$$

$$\phi(\mathcal{X}) = \sum_{n_1=1}^{n_x} U \left((\Psi_\theta^1(\mathcal{X}) S)_{:,n_1} \otimes \psi_\theta^2(x_{n_1}) \right)$$

Because the general polynomial q can be calculated as the sum of monomials, we can summarize the results of the above lemmas to obtain Eq. (5). \square

From the above proposition and

$$\sum_{n_1=1}^{n_x} \sum_{n_2=1}^{n_x} r(S^x)_{n_1 n_2} U(\psi_\theta^1(x_{n_1}) \otimes \psi_\theta^2(x_{n_2})) = \sum_{n_1=1}^{n_x} U \left((\Psi_\theta^1(\mathcal{X}) r(S^x))_{:,n_1} \otimes \psi_\theta^2(x_{n_1}) \right), \quad (12)$$

because of the bilinearity of the Kronecker product, we obtained the approximated feature for the general polynomial.

3.2 Application to matrix square root normalization

In this section, we apply the approximation method obtained in Section 3.1 for matrix square root normalization. Our strategy is to first calculate $b, r(S^x)$ that corresponds to the $1/2$ power of S^x and then substitute these matrices in Eq. (5). Interestingly, we can obtain $b, r(S^x)$ iteratively without calculating the explicit form of the polynomial that corresponds to $1/2$ power.

We first review Newton–Schulz iteration. Given $d \times d$ matrix A that satisfies $\|A - I_d\| < 1$, Newton–Schulz iteration sets $Y_0 = A, Z_0 = I_d$ and then calculates Y_k, Z_k iteratively as follows:

$$Y_{k+1} = \frac{1}{2} Y_k (3I_d - Z_k Y_k) \quad (13)$$

$$Z_{k+1} = \frac{1}{2} (3I_d - Z_k Y_k) Z_k. \quad (14)$$

It is known that Y_k converges to $A^{1/2}$. Furthermore, as shown in this equation, Y_k, Z_k are calculated using only matrix multiplication and summation from A and I_d . This implies that Y_k, Z_k are obtained as the polynomials of A . Moreover, when we view Y_k as the polynomial of A , $Y_0 = A$ and Y_{k+1} is the multiple of Y_k . Thus, the constant term of Y_k is 0. Thus, $b = 0$ holds. Furthermore, we can prove by induction that $Y_k = AZ_k$. This implies that $r(A)$ is obtained as Z_k , and is contrary to the original iSQRT-COV that uses Y_k as the feature.

For a general S^x , as in the case of iSQRT-COV, we normalize S^x as $\frac{1}{\text{trace}(S^x)} S^x$ such that the norm of difference to the identity matrix is smaller than 1. Then, we calculate $r(S^x)$ as $\frac{1}{\sqrt{\text{trace}(S^x)}} Z_k$. The calculation of trace requires only matrix multiplication and summation. We summarize our algorithm in Algorithm 3. We call our method improved polynomial compact covariance pooling (iPCCP).

3.3 Computational Complexity

In this section, we calculate the complexity of the proposed pooling method. We assume the local feature dimension as d , the number of local feature as n , and the global feature dimension as D . When we use the tensor sketch and random Macraulin approximations, the computation of $\Psi_\theta^i(\mathcal{X})$ requires

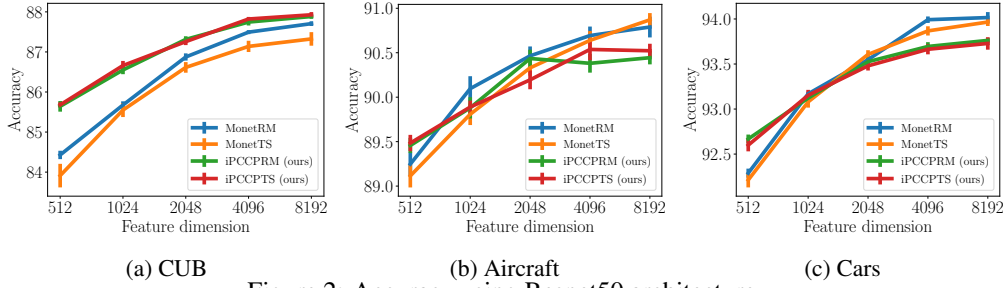


Figure 2: Accuracy using Resnet50 architecture.

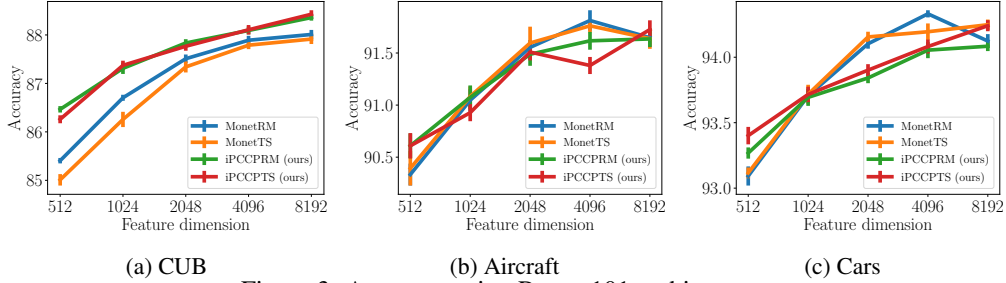


Figure 3: Accuracy using Resnet101 architecture.

$O(nd + nD \log D)$ and $O(ndD)$, respectively. Furthermore, the computation of S requires $O(n^2d + n^3)$, and $\Psi_\theta^1(\mathcal{X})S$ requires $O(n^2D)$. The total complexity is $O(nD \log D + n^2d + n^3 + n^2D)$ for the tensor sketch and $O(ndD + n^2d + n^3 + n^2D)$ for the random Macraulin. In ordinary cases, we can assume $d \simeq n \ll D < d^2 \simeq n^2$. Therefore, the computational complexities for both the pooling methods are equivalent to $O(n^2D)$ for the tensor sketch and $O(ndD + n^2D)$ for the random Macraulin. Owing to the calculation of S , iPCCP with the tensor sketch approximation is slightly slower than the compact bilinear pooling[3] utilizing the same approximation $O(nd + nD \log D)$. Meanwhile, when the random Macraulin approximation is employed, the computational complexity of iPCCP is asymptotically equal to that of the compact bilinear pooling $O(ndD)$.

4 Experiment

In this section, we evaluate the classification accuracy of the proposed method on standard fine-grained image recognition datasets.

We evaluate the methods on the Caltech-UCSD Birds (CUB) [19], FGVC-Aircraft Benchmark (Aircraft) [15], and Stanford Cars (Cars) datasets [9]. The CUB dataset is a dataset consisting of 200 categories bird images with 5,994 training images and 5,794 test images. The Aircraft dataset is a fine-grained airplane image dataset of 100 categories with 6,667 training images and 3,333 test images. The Cars dataset consists of 196 categories of car images with 8,144 training images and 8,041 test images.

We used pretrained Resnet50 and 101 [5] architectures as local feature extractors. To obtain pretrained models that are appropriate for covariance pooling, we pretrained the model that replaced global average pooling with iSQRT-COV [10]. The pretrained setting of iSQRT-COV Resnet was based on [10]. We used the ILSVRC2012 dataset [2] with random clipping and random horizontal flipping augmentations. We set the batch size to 160 and weight decay rate to $1e-4$, and used a momentum grad optimizer with an initial learning rate 0.1 and momentum 0.9 for 65 epochs. We multiplied the learning rate by 0.1 at 30, 45 and 60 epochs.

Based on the pretrained model, we changed the pooling method to iSQRT-COV, Monet, and iPCCP, and compared the accuracy of the fine-tuned models. To match the local features, we used Monet on the covariance. This corresponds to Monet-2 in [4]. We varied the approximation method to random Macraulin and tensor sketch, and approximated the dimensions as 512, 1,024, 2,048, 4,096, and 8,192 for Monet and iPCCP.

Table 2: Accuracy comparison with iSQRT-COV. The score with “(reported)” denotes the score reported in the original paper [10].

Method	Dim	Resnet50			Resnet101		
		CUB	Aircraft	Cars	CUB	Aircraft	Cars
iSQRT-COV (reported) [10]	32k	88.1	90.0	92.8	88.7	91.4	93.3
iSQRT-COV [10]	32k	87.96±0.03	90.69±0.08	93.62±0.03	88.08±0.07	92.05±0.07	93.96±0.05
Monet-TS [4]	8k	87.32±0.17	90.87±0.08	93.97±0.04	87.92±0.10	91.64±0.10	94.25±0.04
Monet-RM [4]	8k	87.71±0.06	90.79±0.12	94.02±0.06	88.01±0.09	91.65±0.09	94.12±0.05
iPCCP-TS (ours)	8k	87.93±0.07	90.52±0.08	93.73±0.07	88.43±0.08	91.73±0.09	94.24±0.04
iPCCP-RM (ours)	8k	87.88±0.06	90.44±0.07	93.76±0.03	88.36±0.06	91.64±0.08	94.08±0.04

Table 3: Comparison time (s) to calculate training/evaluation computation for one minibatch.

Network	iSQRT-COV	Monet-RM	iPCCP-RM (ours)
Resnet50	0.16 / 0.05	0.59 / 0.52	0.24 / 0.08
Resnet101	0.23 / 0.08	0.71 / 0.53	0.32 / 0.10

Following the settings of the existing studies, we resized each input image to 448 x 448 for fine-tuning and evaluation. However, we resized the images to 512 x 512 and cropped the 448 x 448 center image for the Aircraft dataset. Therefore, we obtain a convolutional feature of 28 x 28 x 2,048 dimension as the local feature. We then applied a 1 x 1 convolution layer to reduce the dimension to 28 x 28 x 256 and applied the pooling methods. We applied random horizontal flipping augmentation for fine-tuning, and used the average score for the test image and flipped the test image for evaluation. We set the batchsize as 10 and weight decay rate as 1e-3, and learned the model with momentum grad with learning rates of 1.2e-3 for the feature extractor and 6e-3 for the classifier. We learned the model for 100 epochs.

For each setting, we evaluated the models ten times and evaluated the mean and standard error of the test accuracy.

Figures 2 and 3 show the results. It is noteworthy that the y-axis scale of the CUB is approximately twice as large as that of the other datasets. The proposed method demonstrates comparable performance to Monet. This is because these two methods approximate the same feature. However, our iPCCP demonstrates better performance when the feature dimension is 512 and on the CUB dataset, which dataset demonstrates the lowest accuracy and is thus the most difficult to recognize among the datasets used. We can avoid SVD and approximate the covariance stably using our method; this contributes to learning the discriminative feature even for difficult settings. Furthermore, we compared the score for the 8,192-dimensional feature with iSQRT-COV. Table 2 shows that our methods obtain scores similar to that using iSQRT-COV in all the settings with approximately 1/4 feature dimension.

Furthermore, we compared the computation time. Because the tensor sketch approximation is more complex and the computation time varies significantly according to the implementation, we evaluated the time for the random Macraulin approximation. We compared iSQRT-COV with Monet and the proposed iPCCP for a 8,192-dimensional feature. We implemented each method using pytorch on NVIDIA Tesla V100 and compared the time to calculate the training/evaluation for one minibatch.

Table 3 shows that iPCCP-RM requires a longer computation time than iSQRT-COV arising from the additional computation described in Section 3.3. This additional time is almost the same as the overhead to change the architecture from Resnet50 to Resnet101 and, thus, is not too large to incur difficulty in training and evaluation. Monet required more than twice as long a time compared with iPCCP for training and five times for evaluation. That Monet required a significant amount of time for both training and evaluation could be attributed to the SVD required for forward computation.

The above results demonstrate that the proposed iPCCP is an effective approximation method for an improved covariance feature.

5 Conclusion

We herein proposed a novel direct approximation for covariance features with matrix square root normalization. We applied the fact that the recently proposed Newton–Schulz Iteration-based method approximates the matrix square root as the polynomial of an input covariance matrix, and constructed

the approximation for the matrix square root from the approximation for the general polynomial of a covariance matrix. We evaluated the proposed approximation method on fine-grained image recognition datasets and demonstrated a similar accuracy compared with the original feature with fewer dimensions and less time than the existing approximation methods.

Acknowledgements

This work was partially supported by JST CREST Grant Number JPMJCR1403, Japan, and partially supported by JSPS KAKENHI Grant Number JP19176033.

References

- [1] N. Dalal and B. Triggs. Histograms of oriented gradients for human detection. In *CVPR*, 2005.
- [2] J. Deng, W. Dong, R. Socher, L.-J. Li, K. Li, and L. Fei-Fei. ImageNet: A Large-Scale Hierarchical Image Database. In *CVPR*, 2009.
- [3] Y. Gao, O. Beijbom, N. Zhang, and T. Darrell. Compact bilinear pooling. In *CVPR*, 2016.
- [4] M. Gou, F. Xiong, O. Camps, and M. Sznajder. Monet: Moments embedding network. In *CVPR*, 2018.
- [5] K. He, X. Zhang, S. Ren, and J. Sun. Deep residual learning for image recognition. In *CVPR*, 2016.
- [6] N. J. Higham. *Functions of matrices: theory and computation*, volume 104. Siam, 2008.
- [7] C. Ionescu, O. Vantzos, and C. Sminchisescu. Matrix backpropagation for deep networks with structured layers. In *ICCV*, 2015.
- [8] P. Kar and H. Karnick. Random feature maps for dot product kernels. In *AISTATS*, 2012.
- [9] J. Krause, M. Stark, J. Deng, and L. Fei-Fei. 3d object representations for fine-grained categorization. In *ICCV*, 2013.
- [10] P. Li, J. Xie, Q. Wang, and Z. Gao. Towards faster training of global covariance pooling networks by iterative matrix square root normalization. In *CVPR*, 2018.
- [11] P. Li, J. Xie, Q. Wang, and W. Zuo. Is second-order information helpful for large-scale visual recognition? In *ICCV*, 2017.
- [12] T.-Y. Lin and S. Maji. Improved bilinear pooling with cnns. In *BMVC*, 2017.
- [13] T.-Y. Lin, A. RoyChowdhury, and S. Maji. Bilinear cnn models for fine-grained visual recognition. In *ICCV*, 2015.
- [14] D. G. Lowe. Distinctive image features from scale-invariant keypoints. *IJCV*, 60(2):91–110, 2004.
- [15] S. Maji, J. Kannala, E. Rahtu, M. Blaschko, and A. Vedaldi. Fine-grained visual classification of aircraft. Technical report, 2013.
- [16] N. Pham and R. Pagh. Fast and scalable polynomial kernels via explicit feature maps. In *KDD*, 2013.
- [17] K. Simonyan and A. Zisserman. Very deep convolutional networks for large-scale image recognition. In *ICLR*, 2015.
- [18] Q. Wang, P. Li, and L. Zhang. G2denet: Global gaussian distribution embedding network and its application to visual recognition. In *CVPR*, 2017.
- [19] P. Welinder, S. Branson, T. Mita, C. Wah, F. Schroff, S. Belongie, and P. Perona. Caltech-ucsd birds 200. Technical Report CNS-TR-201, Caltech, 2010.